DOI: 10.1002/adsc.200800035

# Carbon-Carbon Double Bond *versus* Carbonyl Group Hydrogenation: Controlling the Intramolecular Selectivity with Polyaniline-Supported Platinum Catalysts

Martin Steffan,[a] Florian Klasovsky,[a] Jürgen Arras,[a] Christina Roth,[b] Jörg Radnik,[c] Herbert Hofmeister,[d] and Peter Claus[a,*]

[a] Department of Chemistry, Ernst-Berl-Institute, Darmstadt University of Technology, Petersenstr. 20, 64287 Darmstadt, Germany
Fax: (+49)-6151-164-4788; e-mail: claus@ct.chemie.tu-darmstadt.de
[b] Institute for Materials Science, Darmstadt University of Technology, Petersenstr. 23, 64287 Darmstadt, Germany
[c] Leibniz Institute for Catalysis Berlin, Richard-Willstätter-Str. 12, 12489 Berlin, Germany
[d] Max-Planck-Institute of Microstructure Physics Halle, Weinberg 2, 06120 Halle, Germany

Received: January 18, 2008; Revised: February 20, 2008; Published online: May 9, 2008

**Abstract:** The use of polyaniline (PANI) as catalyst support for heterogeneous catalysts and their application in chemical catalysis is hitherto rather poorly known. We report the successful synthesis of highly dispersed PANI-supported platinum catalysts (particle sizes between 1.7 and 3.7 nm as revealed by transmission electron microscopy, TEM) choosing two different approaches, namely (i) deposition-precipitation of $H_2PtCl_6$ onto polyaniline, suspended in basic medium (*DP method*) and, (ii) immobilization of a preformed nanoscale platinum colloid on polyaniline (*sol-method)*. The PANI-supported platinum catalysts were applied in the selective hydrogenation of the α,β-unsaturated aldehyde citral. In order to benchmark their catalytic performance, citral hydrogenation was also carried out by using platinum supported on the classical support materials silica ($SiO_2$), alumina ($Al_2O_3$), active carbon and graphite. The relations of the structural characteristics and surface state of the catalysts with respect to their hydrogenation properties have been probed by EXAFS and XPS. It is found that the DP method yields chemically prepared $PtO_2$ on polyaniline and, thus, produces a highly dispersed and immobilized Adams catalyst (in the β-$PtO_2$ form) which is able to efficiently hydrogenate the conjugated C=C bond of citral (selectivity to citronellal = 87%), whereas reduction of the C=O group occurs with polyaniline-supported platinum (selectivity to geraniol/nerol = 78%) prepared *via* the sol-method. The complete reversal of the selectivity between the preferred hydrogenation of the conjugated C=C or C=O group is not only particularly useful for the selective hydrogenation of α,β-unsaturated aldehydes but also unveils the great potential of conducting polymer-supported precious metals in the field of hitherto barely investigated chemical catalysis.

**Keywords:** Adams catalyst; citral hydrogenation; platinum catalyst; polyaniline

## Introduction

In chemical synthesis heterogeneous hydrogenation catalysts are most useful for the reduction of various functional groups and, thus, are widely applied in industrial processes where the selective hydrogenation of α,β-unsaturated aldehydes is one of the most important reactions, especially for fine chemicals.[1] Citral (3,7-dimethyl-2,6-octadienal) belongs to this class of organic compounds and has three unsaturated bonds (a conjugated system comprised of C=C and C=O groups as well as an isolated C=C bond). Citral hydrogenation leads to industrially important compounds, for example, for the perfumery and flavoring industry. In particular, citronellal is formed by hydrogenation of the olefinic bond which is conjugated to the C=O group whereas hydrogenation of the latter yields the unsaturated, allyl-type alcohols in the *trans* and *cis* forms (geraniol and nerol, respectively). Under certain reaction conditions and depending on the catalyst type, consecutive hydrogenation reactions can occur leading to citronellol, dihydrocitronellal and 3,7-dimethyloctanol (Scheme 1). The selectivity (C=O *vs.* C=C group hydrogenation) can often be controlled by the nature of the individual metal, the presence of a second metal (bimetallic catalysts), metal particle size (dispersion), electron-donating or -withdrawing ligand effects induced by the catalyst

  

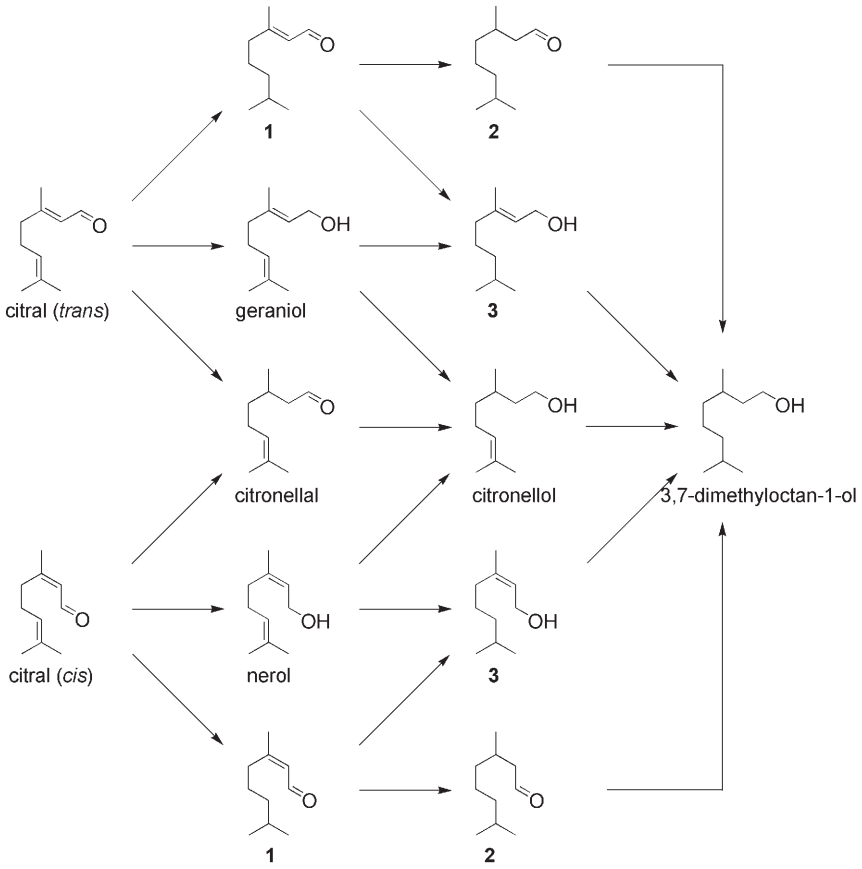


**Scheme 1.** Reaction network of citral hydrogenation, 3,7-dimethyl-2-octenal (**1**), dihydrocitronellal (**2**), 3,7-dimethyl-2-octenol (**3**).

support material, steric constraints in the metal environment and strong metal-support interactions (SMSI). The influence of the above-mentioned parameters on activity and selectivity of catalysts for the selective hydrogenation of α,β-unsaturated aldehydes has been recently reviewed[2,3] and can also be found in numerous studies of citral hydrogenation over supported metal catalysts in the past years (e.g.[4]).

Usually, such hydrogenation reactions are run over group VIII metals which are deposited on classical supports, for example, on oxides ($SiO_2$, $Al_2O_3$, $TiO_2$, zeolites) or activated carbon. Among the various standard preparation procedures which can be applied for supported catalysts, deposition-precipitation, incipient-wetness or preformed metal colloids as precursors[5] are frequently used. More sophisticated methods which allow controlled routes of catalyst synthesis are the heterogenization of organometallic compounds onto the surface of zerovalent metallic particles or highly divided inorganic oxides (surface organometallic chemistry[6]) and the immobilization of metal complexes onto insoluble organic matrices such as polymers.[7] Among the latter, the electrically conducting polymer (ECP) polyaniline (PANI) represents a compound which is easily accessible from low cost feedstock;[8] the synthesis of the intrinsically conductive macromolecule was described manifold in the literature.[9] PANI is of strong interest because of its environmental stability, large conductivity range, good thermal stability and, especially in doped state, high resistance against common solvents; in this respect, it should be an appropriate support material for catalytic processes in gas and liquid phases. The most interesting property of PANI is that, depending on the oxidation state of the aniline polymers, several different forms may arise, which all derive from the basic structure given in Scheme 2. The average oxidation state can vary from fully oxidized ($x=0$, "pernigraniline") to fully reduced ($x=1$, "leucoemeraldine"); the term "emeraldine" is used to designate the structure with equal numbers of oxidized (quinonoid) and reduced (benzenoid) units ($x=0.5$).[8c–e] The latter can, as all the other possible structures, exist as a base (semi-

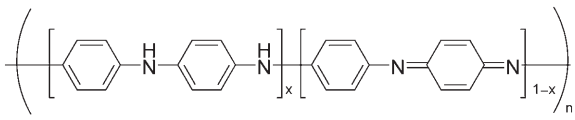

**Scheme 2.** General structure of polyaniline (PANI).

  

conductor) or in the protonated or doped (metallic) form. The transition to the metallic state takes place without any change in the number of electrons; the quinonoid units of the emeraldine salt are converted to benzenoid units by a proton-induced spin-unpairing mechanism that leads to two unpaired electrons.[10]

In the previously published works concerning the synthesis of precious metal-PANI composites[11] the metal was mostly introduced into the bulk of the polymer matrix instead of being deposited on its surface; furthermore, these materials have rarely been used as heterogeneous catalysts for chemical transformations so far. Single examples in this regard are immobilized molybdenum and vanadium complexes[12] for the oxidation of alcohols, the application of W-, V-, Ti- and Mo-PANI composites in epoxidation reactions of olefins[13] as well as the use of nanosized Pd in polyaniline for Suzuki–Mijaura and Heck couplings.[14] A broader field where noble metal-PANI systems are used is electrocatalysis,[15] whereas they are only rarely used as hydrogenation catalysts for unsaturated compounds. An exception is the work by Drelinkiewicz et al. about ethylanthraquinone (with Pd/PANI)[16] and Sobczak et al. about hexyne (with Pt/PANI and Pd/PANI) hydrogenation.[17]

The above discussed structures of PANI should, by subtle combination with metal precursor and synthetic route, offer the possibility of a specific design of novel catalysts which could now control the selectivity in hydrogenations of α,β-unsaturated aldehydes. This fundamental consideration, based on the possibility to manipulate a metal's hydrogenation behavior by structural influences of the support material (*via* electronic and/or steric effects, possesses anchor sites to immobilize metal precursors),[3] inspired us to use polyaniline as support material for platinum catalysts and to apply them in the selective hydrogenation of the α,β-unsaturated aldehyde citral. The conjugated polymer polyaniline has the advantage over other polymers (e.g., polystyrene) that the nitrogen atom in the backbone monomer units can anchor platinum through coordination which leads to pre-organized metal-polyaniline complexes and, after appropriate pretreatment of this hybrid material, forms highly dispersed particles. Therefore, it can be anticipated that catalysts prepared by contacting a Pt complex compound with PANI exhibit different catalytic properties compared to those which are synthesized *via* colloidal metal particles immobilized onto polyaniline. For the synthesis of the Pt/PANI catalysts we chose two different approaches, namely on the one hand the precipitation of $H_2PtCl_6$ as Pt precursor onto polyaniline, suspended in basic medium, with subsequent liquid phase treatment using formalin (*deposition-precipitation, DP*) and, on the other hand, the immobilization of preformed nanoscale Pt colloids on polyaniline (*sol-method*). The resulting catalysts were characterized by ICP-OES, TEM, XPS and EXAFS. The applicability of these novel catalysts was compared with conventional Pt catalysts supported on $SiO_2$, $Al_2O_3$ and activated carbon as well as graphite. To the best of our knowledge, no report is available where an attempt was made to control the selectivity of citral hydrogenation by the synthesis approach described using polyaniline as catalyst support.

## Results and Discussion

### Particle Size Characteristics

Catalyst characterization by TEM revealed that both synthetic routes succeed in producing Pt/PANI catalysts with highly dispersed particles. As depicted in Figure 1 for the catalyst which was prepared by deposition-precipitation (Pt/PANI-3), the observable particles are uniformly distributed on polyaniline and are marked by high dispersion [mean particle diameter of $d=(1.9\pm0.5)$ nm] in addition to a very narrow particle size distribution. The same applies for Pt/PANI catalysts synthesized by the sol-method [Table 1, $d=(1.6\pm0.4)$ nm and $(3.7\pm1.4)$ nm, depending on the Pt loading]. It must be noted that the obtained particle size exhibits the smallest average diameter so far reported on PANI. Other synthetic routes to Pt/PANI materials, where Pt was introduced either electrochemically into PANI films, grown also electrochemically from solutions of aniline and $HClO_4$,[11a] or chemically by spontaneous oxidation of aniline by $[PtCl_6]^{2-}$,[11b] gave much larger particle sizes (200 nm–1 μm and max. 0.5–1 μm, respectively). As to the composition of the particles, TEM analysis of Pt/PANI-3 shows a broad set of lattice spacings. Although size-dependent lattice contractions up to 10% are well-known for supported Pt particles,[18] the measured $d$ values could as well be smoothly attributed to hydrated platinum dioxide species ($PtO_2{\cdot}H_2O$).[19]

### Catalytic Properties of PANI-Supported Platinum Catalysts in Citral Hydrogenation

In order to benchmark their catalytic performance, the Pt/PANI catalysts as well as platinum on the classical support materials $SiO_2$, $Al_2O_3$, activated carbon (AC) and graphite (G) were tested in citral hydrogenation. The results of all catalysts are summarized in Table 1. Since the hydrogenation of citral proceeds *via* a complex reaction network consisting of consecutive and parallel reaction steps (Scheme 1), selectivity data (geraniol/nerol and citronellal from carbonyl and C=C group hydrogenation, respectively) have to be compared at the same conversion level of citral for which $X_{citral}=30\%$ was chosen (Table 1, data were ex-

  

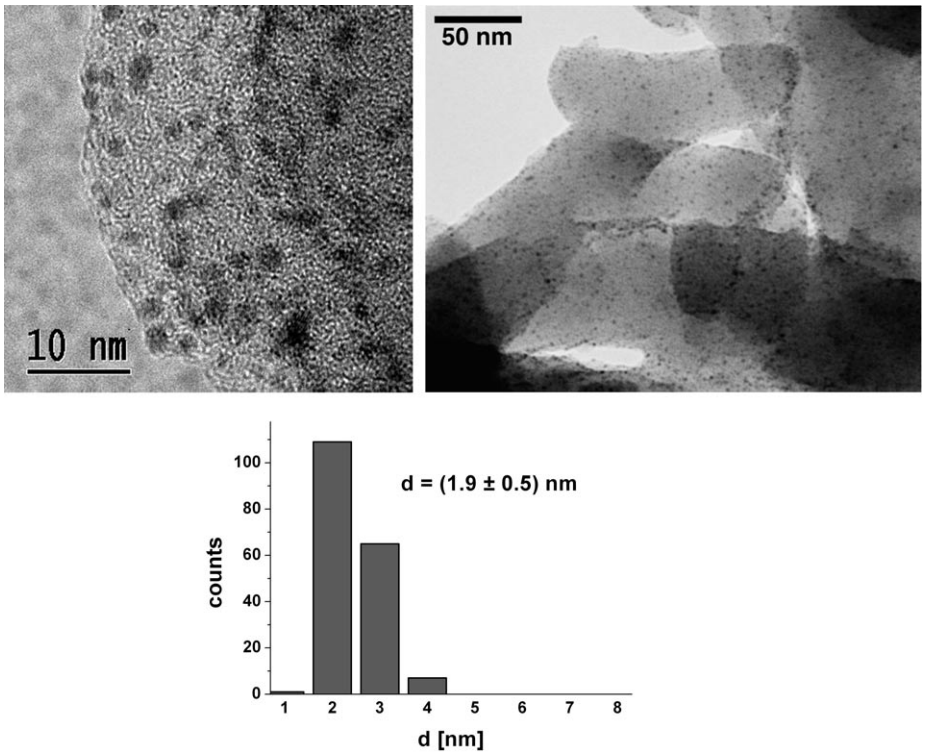


**Figure 1.** TEM images (*top*) and particle size distribution (*bottom*) of Pt/PANI-3.

**Table 1.** Results of citral hydrogenation with polyaniline supported Pt catalysts (Pt/PANI) and Pt on classical supports (platinum particle size, $d_{Pt}$, according TEM), reaction conditions: $T = 140\,°C$, $p(H_2) = 70$ bar, $m_{Kat} = 1.5$ g, $c_0(\text{citral}) = 0.56$ mol/L, solvent: *n*-hexane; all selectivities ($S$) at equal conversion $X_{citral} = 30\%$).

| Entry | Catalyst | Metal content [wt%] | Synthesis route | Pt precursor | Additive | $d_{Pt}$ [nm] | $t_{30}$[a] [min] | $S_{C=O}$[b] [%] | $S_{C=C}$[c] [%] | $S_{SOP}$[d] [%] |
|---|---|---|---|---|---|---|---|---|---|---|
| 1 | Pt/PANI-1 | 2.7 | Sol | $Na_2PtCl_4$ | THPC[e] | $1.6 \pm 0.4$ | 120 | 75 | 20 | 5 |
| 2 | Pt/PANI-2 | 5.0 | Sol | $Na_2PtCl_4$ | THPC | $3.7 \pm 1.4$ | 205[f] | 78 | 19 | 3 |
| 3 | Pt/PANI-3 | 5.0 | DP | $H_2PtCl_6$ | HCHO | $1.9 \pm 0.5$ | 110 | 4 | 87 | 9 |
| 4 | Pt/PANI-4[g] | 4.1 | DP | $H_2PtCl_6$ | HCHO | $1.7 \pm 0.5$ | 225 | 4 | 80 | 16 |
| 5 | Pt/G[h] | 5.0 | - | - | - | - | 30 | 63 | 23 | 14 |
| 6 | $Pt/SiO_2$ | 5.0 | IW | $Pt(NH_3)_4(NO_3)_2$ | $H_2$[i] | - | 60 | 60 | 30 | 10 |
| 7 | $Pt/Al_2O_3$-1 | 5.0 | DP | $H_2PtCl_6$ | HCOONa | $2.8 \pm 0.7$ | 12 | 43 | 46 | 11 |
| 8 | $Pt/Al_2O_3$-2 | 5.0 | Sol | $Na_2PtCl_4$ | THPC | - | 30 | 24 | 49 | 27 |
| 9 | Pt/AC[j] | 5.0 | DP | $H_2PtCl_6$ | HCHO | - | 36 | 24 | 44 | 32 |

[a] Time necessary for $X_{citral} = 30\%$.
[b] Geraniol + nerol.
[c] Citronellal.
[d] Sum of other products (citronellol, isopulegol, dihydrocitronellal, non-identified products).
[e] Tetrakis(hydroxymethyl)phosphonium chloride.
[f] $T = 120\,°C$, $p(H_2) = 50$ bar, $m_{cat} = 1.0$ g.
[g] Own PANI synthesis.
[h] Pt/graphite, commercial product (Alfa).
[i] Followed by treatments in air and $H_2$ (350 °C, 3 h).
[j] Pt/activated carbon.

tracted from the corresponding selectivity-conversion plots). Additionally, the reaction time necessary to obtain a citral conversion of 30% is given as a measure of catalyst activity.

Upon closer examination of the Pt/PANI system, two different selectivity patterns become apparent: (i) the preferential hydrogenation of the carbonyl group of citral leading to the selective formation of the un-

  

saturated alcohols geraniol and nerol ($S_{C=O,\ max} = 78\%$) in the case of Pt/PANI-sol catalysts (Table 1, entries 1 and 2) and (ii) the *complete reversal of the selectivity* towards the selective hydrogenation of the conjugated C=C bond resulting in formation of citronellal ($S_{C=C,\ max} = 87\%$) if Pt/PANI-DP catalysts are used (Table 1, entries 3 and 4). Moreover, considering all support materials applied, the following trend becomes apparent, namely the formation of the allylic alcohols is favored in the sequence Pt/PANI-DP < Pt/AC < $Pt/Al_2O_3$ < $Pt/SiO_2$ < Pt/G < Pt/PANI-sol. For the carbon based catalysts, Pt/G and Pt/AC, the use of graphite as support yields a higher selectivity towards geraniol and nerol compared to activated carbon (Table 1, entries 5 and 9). These results reconfirm the findings of Gallezot[3] for the hydrogenation of cinnamaldehyde with Pt-supported activated carbon and graphite catalysts, respectively. This phenomenon can be interpreted as an electronic ligand effect exerted by the "macroligand"[3] graphite which modifies the local structure of the metal in a two-fold manner: The induced higher charge density on platinum gives rise to a decrease of the binding energy of the C=C bond *via* an increase of the repulsive four-electron interaction and simultaneously favors the backbonding interaction of the antibonding orbital $\pi^*_{CO}$; thus, the carbonyl group hydrogenation is preferred over the C=C bond hydrogenation.[20] The electron-donating properties of the support decrease – analogously to the addition of bases[3] – the probability of the C=C bond hydrogenation which leads to a discrimination between the hydrogenation of the carbonyl group and that of the olefinic bond.

However, this donation effect does not explain the observed complete reversion in selectivity towards citronellal when Pt/PANI-DP was used as catalyst and suggests that, depending on the respective synthetic route, different active sites were generated, which will be discussed as follows.

## In Depth Characterization by XPS and EXAFS/XANES

### X-Ray Photoelectron Spectroscopy

A key to a better understanding offer XPS investigations of the Pt/PANI catalysts, as they are sensitive to the surface and not only provide information about the electronic state of platinum, but also about the nitrogen atoms in the PANI chains.

For all samples C, Pt, N, O and Cl could be detected as components of the outermost region. XPS analysis of both the Pt $4d_{5/2}$ and Pt $4f_{7/2}$ binding energy (BE) in Pt/PANI-2 (prepared by the sol-method) gave values of 316.2 eV and 73.6 eV, respectively (Figure 2). A formal ratio of 1:1.4:4.1 could be estimated for Pt:Cl:O. The binding energy and the composition formally suggest anionic Pt-oxo-chloro-complexes of Pt(II) existing as counterions in the PANI matrix or isolated reduced Pt atoms interacting with the nitrogen containing group of PANI, probably [-NH-]. For isolated Pt atoms on carbon nanotubes Pt $4f_{7/2}$ binding energies of 73.0 eV are described in the literature[21] due to the final state effect. The moderate BE shift of 0.6 eV could be explained by the interaction between the Pt and the substrate. The distinct coloration of the precursor solution after addition of the reducing agent THPC indicates a reduction of the Pt(II) species in the precursor and hereby the existence of Pt(0). It must be noted that such isolated Pt species could not be resolved by TEM. Subsequent treatment with gaseous $H_2$ led to a decrease of the Pt $4d_{5/2}$ binding energy to 315.5 eV whereas the Pt $4f$

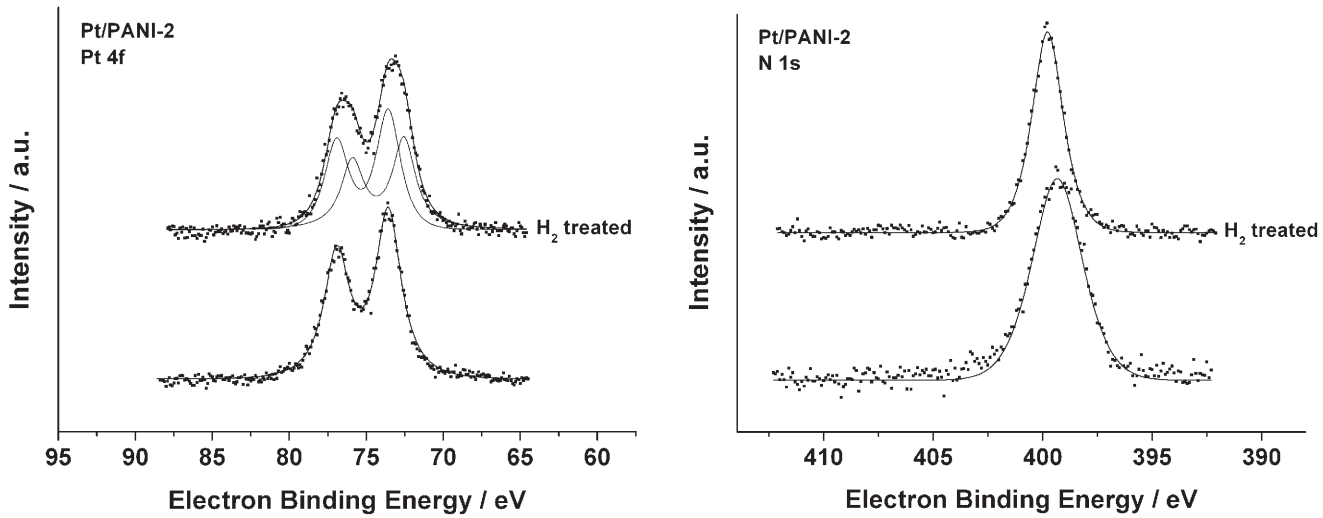


**Figure 2.** Normalized X-ray Pt $4f$ (*left*) and N $1s$ spectra (*right*) of Pt/PANI-2.

  

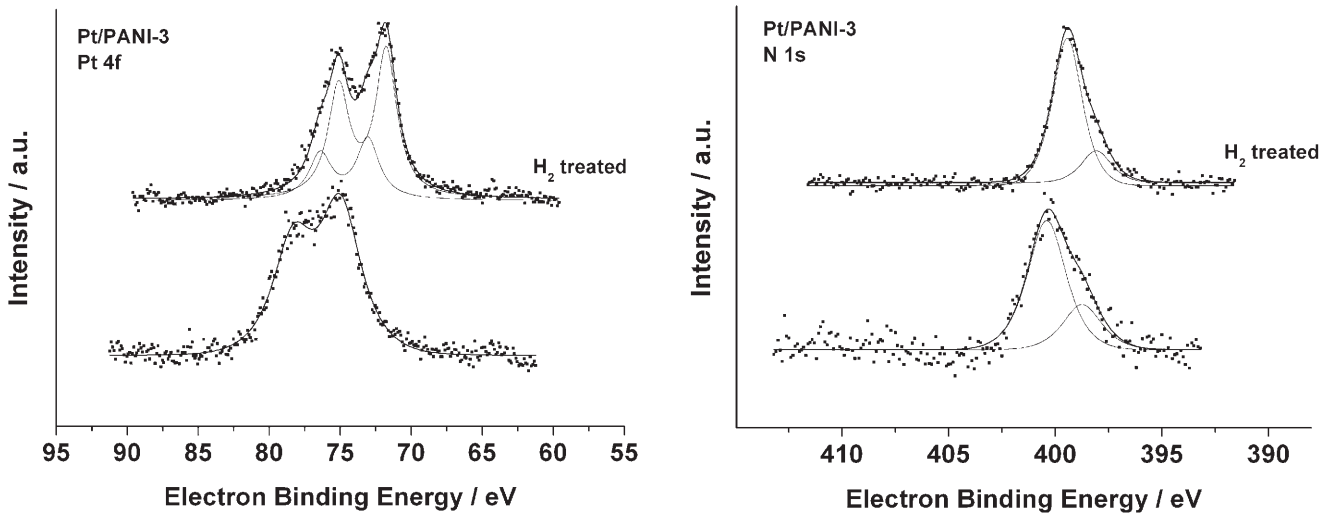


**Figure 3.** Normalized X-ray Pt 4*f* (*left*) and N 1*s* spectra (*right*) of Pt/PANI-3.

peaks can be deconvoluted into two Pt states with a $4f_{7/2}$ BE of 72.4 eV and 73.4 eV, indicating a partial reduction of the platinum (Figure 2). This part is reduced to metallic Pt correlated with the BE of 72.4 eV. This binding energy could be explained by small metallic Pt particles. The second peak at 73.4 eV could be assigned to the reduced Pt-PANI species described formerly, which seems to be stable under the applied hydrogen pre-treatment conditions. The observed N 1*s* binding energy (BE = 399.3 eV, Figure 2), which could be assigned to [-NH-],[10,22] definitely reveals the existence of the benzenoid, fully reduced form of PANI, and this is consistent with the application of the reducing agent THPC during the syntheses. Thus, one could assume that this catalyst, prepared by the sol-method, mostly comprises very small metallic Pt species or even atoms on the *leuco-emeraldine* form (Scheme 2; $x = 1$) of PANI.

A completely different behavior, especially concerning the Pt oxidation state and also with respect to the Pt-N interaction, is found for the XPS analysis of Pt/PANI-3, which was synthesized *via* the deposition-precipitation (DP) method. Here, obviously highly oxidized platinum must dominate as the main component. In fact, the existence of only one valence state of Pt could be concluded from the Pt spectra (Figure 3) with BE of 75.0 eV and 317.2 eV for the Pt $4f_{7/2}$ and $4d_{5/2}$ electrons, respectively, pointing to the presence of platinum oxides ($PtO_2$: Pt $4f_{7/2}$ BE = 74.1–75.6 eV, Pt $4d_{5/2}$ BE = 318.1 eV; *PtO*: Pt $4f_{7/2}$ BE = 72.4–74.6 eV, Pt $4d_{5/2}$ BE = 317.1 eV).[23] The near-surface composition was determined as 1:1:14.7 (Pt:Cl:O).

Furthermore, analysis of the N 1*s* core-level spectrum of Pt/PANI-3 revealed that positively charged nitrogen [-$N^+$-] is present in this catalyst by $^3/_4$ (BE = 400.4 eV, Figure 3).[16,23] The remaining $^1/_4$ of N states measured at a BE of 398.7 eV could not unambiguously be attributed to an imine [=N-] (BE = 398.0 eV)[17,24] or amine [-NH-] nitrogen (BE = 399.5 eV).[17,24]

Taking into account both the Pt 4*f* and N 1*s* spectra, it can be clearly concluded from the XPS analysis of the catalyst Pt/PANI-3 that its surface exclusively consists of highly oxidized platinum which is deposited on the nearly fully oxidized form of PANI, i.e., *pernigraniline* (Scheme 3). In conjunction to the aforementioned TEM results, the visible nanoparticles in this catalyst type consist of hydrated platinum oxide whose water content might be diminished at the outermost shell. Note that during treatment with gaseous $H_2$ a considerable reduction of Pt took place; two states at Pt $4f_{7/2}$ BE = 71.8 eV and BE = 73.2 eV in a ratio of 3:1 could be observed (Figure 3). The former could be correlated with the metallic form, whereas a part of Pt seems to remain as oxide during $H_2$ treatment. At the same time, the N 1*s* binding energy is shifted to a peak which can be deconvoluted to 399.4 eV and 398.1 eV indicating that the nitrogen in PANI presumably exists mainly in the amine form (82%), the imine remains only to a much lesser content (18%). As expected, the amount of chlorine and especially of oxygen decreased during the $H_2$ treatment.

## EXAFS/XANES Studies

To leave no doubt that Pt/PANI-3 catalyst is indeed composed of highly oxidized platinum particles, additional analysis by X-ray absorption fine structure (EXAFS) spectroscopy also gives evidence for this structure.

  

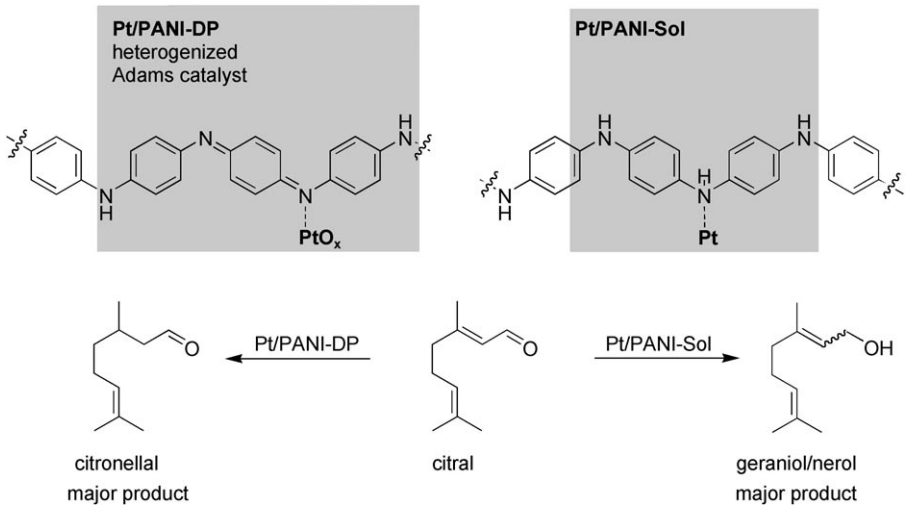


**Scheme 3.** Different interactions between Pt and PANI showing the favored hydrogenation product, Pt-PANI-2 (*right*), Pt/PANI-3 (*left*).

## XANES Analysis

In Figure 4, the XANES region of Pt/PANI-3 has been plotted and compared to a commercial Pt/C catalyst in its as-received state and after exposure to 5% hydrogen in a nitrogen atmosphere at room temperature. The most obvious changes occur both in the white-line and the edge position. In contrast to the hydrogen-reduced, but also to the as-received Pt/C, the white-line intensity of Pt/PANI-3 is significantly enhanced and the Pt $L_3$ absorption edge position is shifted to higher energies indicative of a higher oxidation state. Furthermore, the oscillatory structure in the extended edge region of the spectrum is far less pronounced for Pt/PANI-3 than for Pt/C. Both observations lead us to propose a platinum oxide structure with very small particle sizes for Pt/PANI-3.

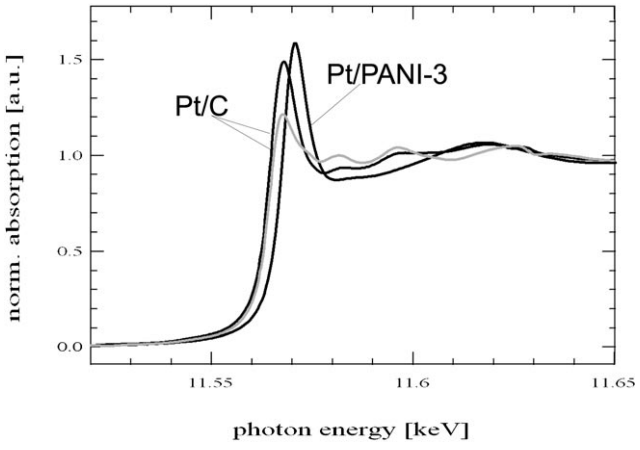


**Figure 4.** Near-edge region of Pt/PANI-3 (black) compared to Pt/C in its as-received state (dark gray) and after reduction at room temperature in 5% hydrogen/$N_2$ flow (light gray).

A comparison with literature data further substantiates the above assumption: XANES spectra reported for $[Pt(H_2O)_4]^{2+}(aq)$[25] appear very similar to that of Pt/PANI-3, whereas only little resemblance seems to be there with $[PtCl_4]^{2-}(aq)$. In particular, the white lines for the aqua complexes are very pronounced with only little structure beyond the absorption edge.

## EXAFS Analysis

In a first step, the raw spectra were background-subtracted, normalized and Fourier transformed. A qualitative comparison of hydrogen-reduced Pt/C and Pt/PANI-3 on the one hand is displayed in Figure 5, while a comparison of as-received Pt/C and Pt/PANI-3 is shown in Figure 6.

Both FTs in Figure 5 look distinctly different. In the case of reduced Pt/C, the most prominent contribution appears at a distance of approximately 2.8 Å, which is consistent with a metallic Pt–Pt distance. For Pt/PANI-3, however, the main feature is centered at about 1.9 Å attributed to a Pt–O contribution. No evidence of a Pt–Cl contribution is observed, which should occur at approximately 2.4 Å according to the literature.[26] The same is true for a comparison of the chi data of Pt/C and Pt/PANI-3 (Figure 6). At values below $k = 5$ Å$^{-1}$ in $k$ space, the data appear almost identical, whereas at higher k values significant differences are observed. In the higher $k$ range, the metallic contribution becomes predominant, and consequently, Pt/PANI-3 seems to be much more oxidized even than Pt/C in its as-received state, which was used as a reference.

The above information was used to generate two different start models for the fitting of the EXAFS data: a) model I including Pt–Pt, Pt–O and an addi-

  

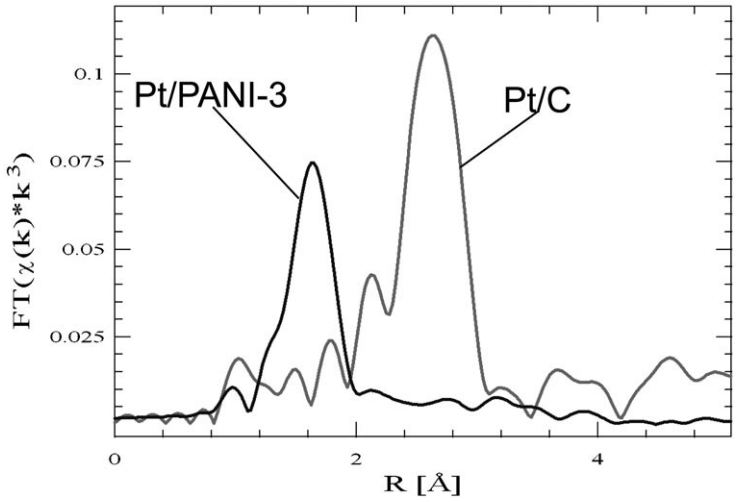


**Figure 5.** FT of Pt/PANI-3 (black) compared to Pt/C after reduction at room temperature in 5% hydrogen/$N_2$ flow (dark gray).

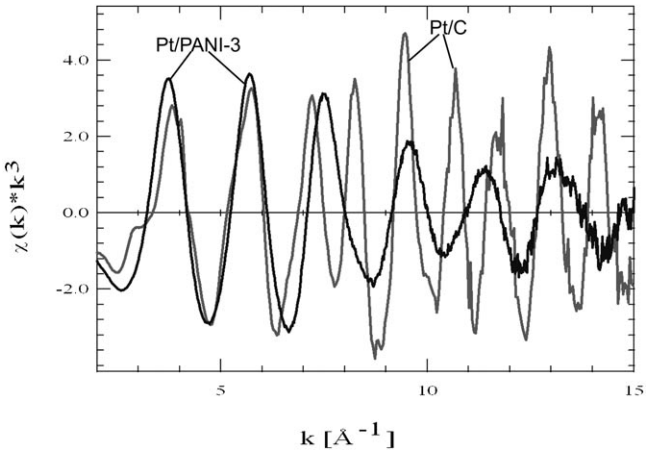


**Figure 6.** Data of Pt/PANI-3 in *k* space (black) compared to Pt/C in its as-received state (dark gray).

tional Pt–Cl coordination and b) model II with Pt–Pt and two Pt–O shells according to β-$PtO_2$ as reported in the literature.[27] Both models were applied to fit the EXAFS data, and the fit parameters are listed in Table 2. In Figure 7, the data in *k* space and the corresponding fit are shown for the sample fitted with model I (Figure 7a) as well as for the sample fitted with model II (Figure 7b).

For model I, Pt–O was found to be the predominant contribution with a coordination number $N_{Pt-O}$ of 4.0 at a standard Pt–O distance of 2.00 Å. Both Pt–Pt and Pt–Cl contributions were less pronounced with coordination numbers of $N_{Pt-Pt}=0.7$ and $N_{Pt-Cl}=0.3$, respectively. Using model II for the fit, the Pt–O shell at a distance of 2.01 Å remains the dominant feature with a coordination number $N_{Pt-O}$ of 4.0, while the second Pt–O shell at 2.18 Å and the Pt–Pt contribution at 3.02 Å are less pronounced ($N_{Pt-Pt}=1.8$ and $N_{Pt-O}=1.4$, respectively). The significantly larger Pt–Pt distance observed is in good agreement with $PtO_2$ data reported in the recent literature.[28] The obtained values are reasonable for both models used. However, the quality of the fit was significantly smaller, when model II was used.

From the X-ray absorption data and in good agreement with the XPS data, it is concluded that the sample consists largely of β-$PtO_2$ with very small particle sizes. $PtO_2$ in bulk form, usually prepared by fusion of $H_2PtCl_6$ with $NaNO_3$ at 450–500 °C, is known in organic synthesis and heterogeneous catalysis as Adams catalyst which exhibits excellent hydrogenation properties.[29] Detailed XRD analysis of

**Table 2.** Summary of the EXAFS results using either model I or model II for the fit; $3 < k < 14$ Å$^{-1}$, $1.5 < R < 3.2$ Å.

| Model | N (±10%) | R [Å] (±0.02) | $\sigma^2$ [Å$^2$] (±5%) | $E_0$ [eV] (±10%) |
|---|---|---|---|---|
| model I | $N_{Pt-Pt}=0.7$ | $R_{Pt-Pt}=2.77$ | 0.006 | −15.0 |
| | $N_{Pt-O}=4.0$ | $R_{Pt-O}=2.00$ | 0.006 | 3.0 |
| | $N_{Pt-Cl}=0.3$ | $R_{Pt-Cl}=2.50$ | 0.006 | −15.0 |
| model II | $N_{Pt-Pt}=1.8$ | $R_{Pt-Pt}=3.02$ | 0.009 | 6.6 |
| | $N_{Pt-O}=4.0$ | $R_{Pt-O}=2.01$ | 0.003 | −0.4 |
| | $N_{Pt-O}=1.4$ | $R_{Pt-O}=2.18$ | 0.004 | 4.7 |

  

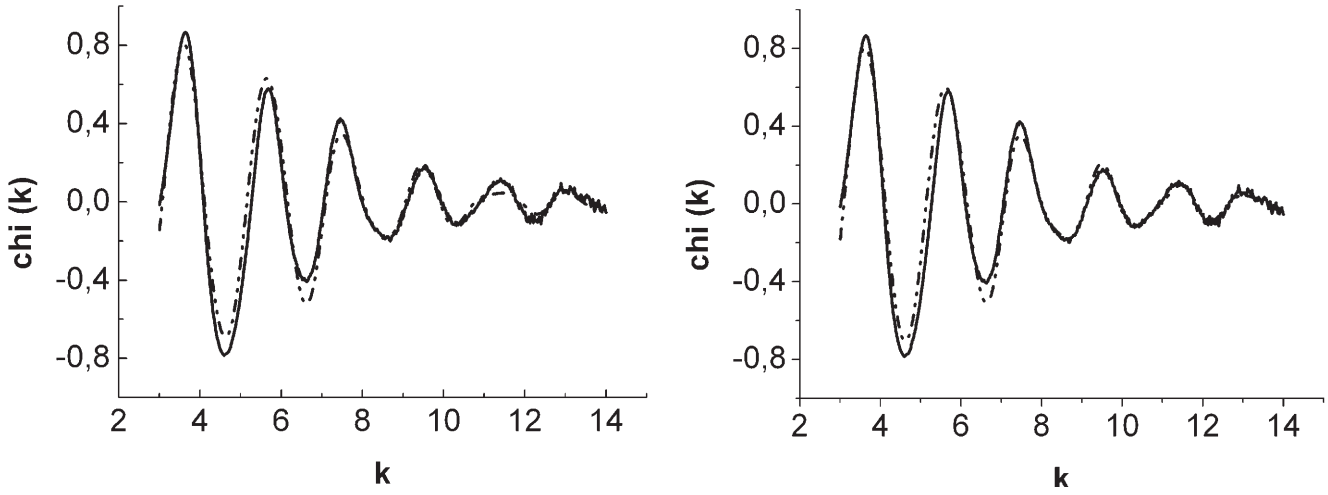


**Figure 7.** Chi data and fit for Pt/PANI-3; fit obtained when using model I including a Pt–Cl contribution (*left*), data fitted with model II for β-$PtO_2$ (*right*).

Adams catalysts revealed that they are a mixture of α-$PtO_2$ as main component besides Pt and platinum bronze ($Na_xPt_3O_4$). Proof of the latter is a clear hint for introducing sodium into the platinum oxide which may affect the hydrogenation properties of the Adams catalyst. The preparation method applied in the present study constitutes a simple and new way to fabricate an immobilized Adams catalyst (in the β-$PtO_2$ form) which is an efficient C=C group hydrogenation catalyst (Table 1). It is assumed that the reduction of β-$PtO_2$ easily occurs in the presence of polyaniline (see Figure 3 and the associated discussion in the XPS part) fabricating highly dispersed, PANI-supported platinum black under the reaction conditions. These distinct platinum clusters could now interact with the conjugated C=C bond, resulting in the formation of citronellal.

Although information about selective hydrogenation with polyaniline-supported precious metal catalysts and especially regarding supported nanodispersed Adams catalysts is very limited, there are a few hints which support the findings of the present study. The strong catalytic activity of the novel immobilized platinum oxide towards C=C group hydrogenation is in line with the increased surface reactivity of polyaniline-supported $[PdCl_4]^{2-}$ complexes towards the hydrogenation of olefins and alkynes compared to Pd(0).[17] On the other hand, a commercial (bulk) Pt-Adams catalyst exhibiting either large agglomerates of 2–5 nm crystallites when reduced at 333 K or large facetted particles in the size range 20–200 nm due to extensive sintering and recrystallization at a reduction temperature of 373 K was used for cinnamaldehyde hydrogenation.[30] The large particles were more selective towards the carbonyl group hydrogenation yielding cinnamyl alcohol whereas the C=C bond was hydrogenated much more rapidly in the case of smaller particles, that is, selectivity has been found to be structure-sensitive in that case. According to the results of the present study, polyaniline seems to take the role of the charge density donor, in line with the works of Kaner et al.,[31] and, thus, is a suitable support for selective citral hydrogenation towards the unsaturated alcohols *provided* that metallic platinum particles are present which have been prepared from preformed colloids in the present study (Pt/PANI-2). Then, electron transfer from PANI to Pt allows an increase of the hydridic character of the chemisorbed hydrogen and, thus, the rate of the nucleophilic addition of $H^-$ on the positively charged carbon of the carbonyl group is enhanced.

The reducibility of the highly oxidized Pt species is increased due to strong interaction with the PANI support. Further catalyst characterization by electron spin resonance (ESR) should also confirm the presence of easily reducible, highly oxidized Pt species, which are able to withdraw electron density and deplete the number of polarons in the PANI support due to strong interaction.

## Conclusions

In the present article the applicability of chemically synthesized platinum/polyaniline catalysts for selective hydrogenation of the α,β-unsaturated aldehyde citral was presented and the role of different platinum species affecting selectivity elucidated. It is found that supporting chemically prepared $PtO_2$ on polyaniline produces a highly dispersed, supported Adams catalyst which is able to efficiently hydrogenate the conjugated C=C bond of citral whereas reduction of the carbonyl group occurs with polyaniline-supported Pt. This approach, hitherto not described in the literature,

  

is not only particularly useful for the selective hydrogenation of α,β-unsaturated aldehydes by controlling the selectivity of this also industrially significant reaction, but also unveils the great potential of conducting polymer supported precious metals in the field of hitherto barely investigated chemocatalysis. Precisely in this regard, we expect that polyaniline as support material offers novel alternatives for the rational design of catalysts with desired features – not only for hydrogenations, but also for partial oxidations – the latter remained unused to a large extent so far.

## Experimental Section

### Catalysts Synthesis and Characterization

The graphite-supported catalyst 5Pt/G was a commercial product (Alfa Aesar); other materials used for preparation were obtained from Chempur ($Na_2PtCl_4$), Merck {tetrakis-(hydroxymethyl)phosphonium chloride [THPC], formaldehyde [37 wt%], NaOH}, Aldrich {polyaniline [PANI, $M_w$ = 65.000], $Pt(NH_3)_4(NO_3)_2$}, LaRoche (alumina [Versal GL25]), Fluka (sodium formate [HCOONa]), Heraeus ($H_2PtCl_6$ solution), Alfa Aesar (large pore silica) and Arkema (activated carbon [AC, Acticarbone]).

The synthesis of the catalysts Pt/PANI-1, Pt/PANI-2 and $Pt/Al_2O_3$-2 was carried out using preformed Pt colloids which were prepared according to a modified sol-method.[5] After immobilization onto the supports, the materials were used as catalysts without any further treatment. More precisely, for the preparation of Pt/PANI-1 an aqueous solution of $Na_2PtCl_4$ (0.5 g in 100 mL $H_2O$) was combined with a solution of THPC (2.5 mL, 1.3 wt%) and NaOH (3.75 mL, 0.2 mol/L) in water (117.5 mL). After 1 h aging time, the as-prepared sol was added to a suspension of 10 g PANI in 1 L $H_2O$, stirred overnight, filtered, washed (50 mL $H_2O$) and dried (110 °C, 2.5 h). The intermediate Pt/PANI composite thus obtained was loaded with a second sol portion as described above. Pt/PANI-2 was prepared in a one-step immobilization using a sol derived from an $Na_2PtCl_4$ (0.4 g in 40 mL $H_2O$) and a THPC solution (3 mL 0.2 mol/L NaOH, 4 mL 1.3 wt% THPC, 94 mL $H_2O$), whereas in the case of $Pt/Al_2O_3$-2, 4.75 g alumina, suspended in 500 mL water, served as support for a sol prepared according to Pt/PANI-1.

During the preparation of Pt/PANI-3, Pt/PANI-4, Pt/AC and $Pt/Al_2O_3$-1 *via deposition-precipitation*, 9.5 g of support were suspended in 50 mL diluted aqueous $Na_2CO_3$ (10 wt%). The suspensions were combined with 20 mL $H_2PtCl_6$ solution (containing 0.5 g Pt) and stirred for 15 min at 90 °C with a pH maintained neutral by further addition of aqueous $Na_2CO_3$. After addition of (i) a mixture containing formaldehyde solution and NaOH solution (10 wt%) in a volume ratio of 4.8/1 (for PANI and AC supports) or (ii) a dilute HCOONa solution (for alumina support), the suspensions were stirred for further 20 min, filtered, washed and dried in air overnight.

$Pt/SiO_2$ was obtained *via incipient-wetness impregnation* of the support (4.75 g, pre-dried at 250 °C for 2.5 h) with a 0.5 g portion of $Pt(NH_3)_4(NO_3)_2$ (Aldrich) dissolved in 9.5 mL water. After drying (room temperature overnight, then at 80 °C for 2 h), the catalyst was calcined in air and reduced in flowing hydrogen at 350 °C for 3 h.

The catalysts were characterized by several methods. The metal content was estimated by ICP-OES (Perkin–Elmer Optima 3000XL) after dissolving the materials in a mixture of $HF/HNO_3$ by means of a MDS-2000 microwave unit (CEM).

The size of the polyaniline-supported particles and their morphology was determined by transmission electron microscopy, TEM (JEOL JEM-3010, 300 kV, $LaB_6$-cathode).

X-ray photoelectron spectroscopy (XPS) has been applied to obtain information on the chemical environment of surface atoms, in particular the oxidation state of platinum loaded to the PANI support and the chemical state of the PANI nitrogen. Surface analytical measurements were performed by means of a VG ESCALAB 220 iXL spectrometer with an Mg $K_\alpha$ radiation source. The C 1*s*-peak at 284.8 eV was used as a reference for the binding energy. After satellite and background subtraction the peaks were fitted with Gaussian–Lorentzian curves. The peak positions could be determined with a precision of ±0.1 eV. The quantitative composition was elucidated from the peak areas, which were divided by the transmission function of the spectrometer and element specific Scofield factors.

To elucidate the chemical nature of platinum and to obtain quantitative structural information, we carried out X-ray absorption fine structure (EXAFS) spectroscopy. The X-ray absorption spectrum of the Pt $L_3$-edge was obtained at the beamline X1 at Hasylab, Hamburg, with the synchrotron source operated at an energy of 4.45 GeV and an initial positron beam current of 120 mA. The measurements were carried out in transmission mode in an energy range from $E$ = 11300 eV up to 12800 eV (Pt $L_3$-edge at 11564 eV), using a thin Pt metal foil as reference. An Si(111) double-crystal monochromator was used and detuned to 50% intensity to avoid higher harmonics present in the X-ray beam. The intensities of the focused beam and the transmitted beam were detected by three gas-filled ion chambers in series. Extraction of the EXAFS data from the measured raw data was either performed with the program package WinXAS[32] (for qualitative comparison only) or the XDAP code developed by Vaarkamp et al.[33] The pre-edge was approximated by a modified Victoreen curve, and normalization was carried out by dividing the absorption spectrum by the height of the absorption edge at 50 eV above the edge.[34,35] The background was approximated by a spline function defined by:

$$\sum_{i=1}^{NPTS} \frac{(\mu_i - BCK_i)^2}{e^{-WEk_i^2}} \leq SM$$

with SM = smoothing parameter. The data as finally shown in this paper were obtained with a multiple shell R-space fit with $k^1$ weighting, $\Delta k$ = 3.0–14 $Å^{-1}$ and $\Delta R$ = 1.4–3.2 Å. To obtain the final fit, all parameters were fully optimized in $k^0$, $k^1$, $k^2$ and $k^3$ weighting. Theoretical phase shifts and backscattering amplitudes for the Pt–Pt, Pt–Cl and Pt–O absorber-scattering pairs were used in EXAFS data analy-

  

sis,[36] which were generated utilizing the FEFF7 code.[34] Sample preparation was done by diluting 180 mg of the powder sample in 200 mg of boronitride and pressing it into a dense pellet (calculated to have an absorbance of 1.5). The pellet was then fixed onto the multiple sample holder, which was cooled down to liquid nitrogen temperature. Two spectra were recorded with recording times of approximately 45 min each and added to improve the spectra quality.

Data analysis was carried out in two steps: first of all, the near-edge region is discussed qualitatively and compared to literature data. In a second step, an EXAFS analysis is performed fitting the Fourier-transformed spectrum to a reasonable model using the software package XDAP.

The near-edge region, FT and data of polyaniline-supported platinum in *k* space are referred to a commercial carbon-supported platinum catalyst (Pt/C) which was purchased from E-TEK.

### Citral Hydrogenation

The catalytic runs were carried out in a stainless steel batch reactor (Parr Instr., 300 mL). The catalyst ($m_{cat}$ = 1–1.5 g) was filled into the reactor before addition of the reaction mixture containing the educt (10 mL citral, Merck), the solvent (90 mL *n*-hexane) and an internal GC standard (5 mL *n*-tetradecane). The mixture was flushed three times with 20 bar argon, and heated under argon pressure to 120 and 140 °C, respectively. After reaching the desired reaction temperature the reactor was charged with hydrogen [$p(H_2)$ = 50 or 70 bar] and the reaction started. Samples were taken periodically and analyzed with temperature programmed, off-line capillary gas chromatography equipped with an Agilent DB-Wax column ($l$ = 30 m, $d_i$ = 0.25 mm, $t_f$ = 0.25 μm).

## Acknowledgements

*P.C. thanks the Fonds der Chemischen Industrie.*

## References

[1] *Ullmann's Encyclopedia of Industrial Chemistry*, Flavors and Fragrances, electronic release, Wiley-VCH, **2005**.

[2] a) P. Claus, *Top. Catal.* **1998**, *5*, 51; b) P. Mäki-Arvela, J. Hajek, T. Salmi, D. Murzin, *Appl. Catal. A: General* **2005**, *292*, 1; c) P. Claus, Y. Önal, *Regioselective Hydrogenation*, in: *Handbook of Heterogeneous Catalysis*, (Eds.: G. Ertl, H. Knözinger, F. Schüth, J. Weitkamp), 2nd edn., Wiley-VCH, Weinheim, **2007**, in press; d) V. Ponec, *Appl. Catal. A: General* **1997**, *149*, 27.

[3] P. Gallezot, D. Richard, *Catal. Rev. Sci. Eng.* **1998**, *40*, 81.

[4] a) S. Mukherjee, M. A. Vannice, *J. Catal.* **2006**, *243*, 108; b) S: Mukherjee, M. A. Vannice, *J. Catal.* **2006**, *243*, 131; c) U. K. Singh, M. A. Vannice, *J. Catal.* **2001**, *199*, 73; d) U. K. Singh, M. N. Sysak, M. A. Vannice, *J. Catal.* **2000**, *191*, 181; e) U. K. Singh, M. A. Vannice, *J. Catal.* **2000**, *191*, 165; f) U. K. Singh, M. A. Vannice, *J. Mol. Catal. A: Chem.* **2000**, *163*, 233; g) P. Centomo, M. Zecca, S. Lora, G. Vitulli, A. M. Caporusso, M. L. Tropeano, C. Milone, S. Galvagno, B. Corain, *J. Catal.* **2005**, *229*, 283; h) C. Milone, R. Ingoglia, S. Galvagno, *Gold Bull.* **2006**, *39*, 54; i) B. Bachiller-Baeza, A. Guerrero-Ruiz, P. Wang, I. Rodriguez-Ramos, *J. Catal.* **2001**, *204*, 450; j) L. Sordelli, R. Psaro, G. Vlaic, A. Cepparo, S. Recchia, C. Dossi, A. Fusi, R. Zanoni, *J. Catal.* **1999**, *182*, 186; k) A. M. Silva, O. A. A. Santos, M. J. Mendes, E. Jordao, M. A. Fraga, *Appl. Catal. A: General* **2003**, *241*, 155.

[5] D. G. Duff, A. Baiker, P. P. Edwards, *Langmuir* **1993**, *9*, 2301.

[6] F. Humblot, D. Didillon, F. Lepeltier, J. P. Candy, J. Corker, O. Clause, F. Bayard, J. M. Basset, *J. Am. Chem. Soc.* **1998**, *120*, 137.

[7] Y. Wang, H. Liu , Y. Huang, *Polym. Adv. Technol.* **1998**, *7*, 634.

[8] a) T. Ito, H. Shirakawa, S. Ikeda, *J. Polym. Sci. Chem. Ed.* **1974**, *12*, 11; b) H. Shirakawa, E. J. Louis, A. G. MacDiarmid, C. K. Chiang, A. J. Heeger, *J. Chem. Soc. Chem. Commun.* **1977**, 578; c) H. Shirakawa, *Angew. Chem.* **2001**, *113*, 2642; *Angew. Chem. Int. Ed.* **2001**, *40*, 2574; d) A. G. MacDiarmid, *Angew. Chem.* **2001**, *113*, 2649; *Angew. Chem. Int. Ed.* **2001**, *40*, 2581; e) A. J. Heeger, *Angew. Chem.* **2001**, *113*, 2660; *Angew. Chem. Int. Ed.* **2001**, *40*, 2591.

[9] Y. Cao, A. Andreatta, A. J. Heeger, P. Smith, *Polymer* **1989**, *30*, 2305.

[10] E. T. Kang, K. G. Neoh, T. C. Tan, S: H. Khor, K. L. Tan, *Macromolecules* **1990**, *23*, 2918.

[11] a) J. M. Kinyanjui, N. R. Wijeratne, J. Hanks, D. W. Hatchett, *Electrochim. Acta* **2006**, *51*, 2825; b) J. M. Kinyanjui, R. Harris-Burr, J. G. Wagner, N. R. Wijeratne, D. W. Hatchett, *Macromolecules* **2004**, *37*, 8745; c) J. A. Smith, M. Josowicz, M. Engelhard, D. R. Baer, J. Janata, *Phys. Chem. Chem. Phys.* **2005**, *7*, 3619; d) K. Mallick, M. J. Witcomb, M. S. Scurrell, *J. Mater. Sci.* **2006**, *41*, 6189.

[12] a) S. R. Reddy, S. Das, T. Punniyamurthy, *Tetrahedron Lett.* **2004**, *45*, 3561; b) S. Velusamy, M. Ahamed, T. Punniyamurthy, *Org. Lett.* **2004**, *6*, 4821.

[13] S. Bischoff, M. Kant, (Institut für Angewandte Chemie Berlin-Adlershof), German Patent DE 10164467, **2003**.

[14] a) B. J. Gallon, R. W. Kojima, R. B. Kaner, P. L. Diaconescu, *Angew. Chem.* **2007**, *119*, 7389; *Angew. Chem. Int. Ed.* **2007**, *46*, 7251; b) M. L. Kantam, M. Roy, S. Roy, B. Sreedhar, S. S. Madhavendras, B. M. Choudary, R. Lal De, *Tetrahedron* **2007**, *63*, 8002; c) A. Houdayer, R. Schneider, D. Billaud, J. Ghanbaja, J. Lambert, *Appl. Organomet. Chem.* **2005**, *19*, 1239; d) B. M. Choudary, M. Roy, S. Roy, M. L. Kantam, B. Sreedhar, K. V. Kumar, *Adv. Synth. Catal.* **2006**, *348*, 1734; e) T. Amaya, D. Saio, T. Hirao, *Tetrahedron Lett.* **2007**, *48*, 2729; f) A. Houdayer, R. Schneider, D. Billaud, J. Ghanbaja, J. Lambert, *Synth. Met.* **2005**, *151*, 165.

[15] a) B. Rajesh, K. Ravindranathan Thampi, J. M. Bonard, H. J. Mathieu, N. Xanthopoulos, B. Viswanathand, *Electrochem. Solid-State Lett.* **2004**, *7*, A404; b) J. Augustynski, P. Kedzierzawski, A. Carroy, *Proc. Electrochem. Soc.* **1996**, *96–98*, 396.

[16] A. Drelinkiewicz, M. Hasik, M. Kloc, *J. Catal.* **1999**, *18*, 123.

  

[17] J. W. Sobczak, A. Kosinski, A. Bilinski, J. Pielaszek, W. Palczewska, *Adv. Mater. Opt. Electron.* **1998**, *8*, 295.
[18] M. Klimenko, S. Nepijko, H. Kuhlenbeck, M. Bäumer, R. Schlögl, H. J. Freund, *Surf. Sci.* **1997**, *391*, 27.
[19] D. Dou, D. J. Liu, W. B. Williamson, K. C. Kharas, H. J. Robota, *Appl. Catal. B: Enviromental* **2001**, *30*, 11.
[20] a) P. Sautet, *Top. Catal.* **2000**, *13*, 213; b) F. Delbecq, P. Sautet, *J. Catal.* **1995**, *152*, 217; c) S. Schimpf, M. Lucas, D. Hönicke, P. Claus, *Chem. Ing. Tech.* **2002**, *74*, 1564.
[21] a) Y. T. Kim, K. Ohshima, K. Higashimine, T. Uruga, M. Takata, H. Suematsu, T. Mitani, *Angew. Chem.* **2006**, *118*, 421; *Angew. Chem. Int. Ed.* **2006**, *45*, 407; b) W. Eberhardt, P. Fayet, D. M. Cox, Z. Fu, A. Kaldor, R. Sherwood, D. Sondericker, *Phys. Rev. Lett.* **1990**, *64*, 780; c) G. K. Wertheim, S. B. DiCenzo, S. E. Youngquist, *Phys. Rev. Lett.* **1983**, *51*, 2310.
[22] A. Bhattacharyya, R. Roy, S. K. Sen, S. Sen, A. K. Chakraborty, T. K. Bhattacharyya, *Pergamon* **1998**, *49*, 253.
[23] NIST X-ray photoelectron spectroscopy database 20, version 3.4, http://sradata.nist.gov./xps/.
[24] J. W. Sobczak, A. Kosinski, A. Jablonski, W. Palczewska, *Top. Catal.* **2000**, *11/12*, 307.
[25] R. Ayala, E. S. Marcos, S. Diaz-Moreno, V. A. Sole, A. M. Paez, *J. Phys. Chem. B* **2001**, *105*, 7588.
[26] B. H. Hwang, C. H. Chen, L. S. Sarma, J. M. Chen, G. R. Wang, M. T. Tang, D. G. Liu, J. F. Lee, *J. Phys. Chem. B* **2006**, *110*, 6475.
[27] A. N. Mansour, D. E. Sayers, J. W. Cook, D. R. Short, R. D. Shannon, J. R. Katzer, *J. Phys. Chem.* **1984**, *88*, 1778.
[28] P. Bera, K. R. Priolkar, A. Gayen, P. R. Sarode, M. S. Hegde, S. Emura, R. Kumashiro, V. Jayaram, G. N. Subanna, *Chem. Mater.* **2003**, *15*, 2049.
[29] a) S. Nishimura, *Handbook of Heterogeneous Catalytic Hydrogenation for Organic Synthesis*, Wiley-Interscience New York, **2001**, p 31; b) R. Augustine, *Heterogeneous Catalysis for the Synthetic Chemist*, Marcel Dekker, Inc., New York, **1996**, p 231.
[30] A. Giroir-Fendler, D. Richard, P. Gallezot, *Catal. Lett.* **1990**, *5*, 175.
[31] a) R. J. Tseng, C. O. Baker, B. Shedd, J. Huang, R. B. Kaner, J. Ouyang, Y. Yang, *Appl. Phys. Lett.* **2007**, *90*, 053101; b) R. J. Tseng, J. Huang, J. Ouyang, R. B. Kaner, Y. Yang, *Nano Lett.* **2005**, *5*, 1077.
[32] Th. Ressler, *J. de Physique IV* 7, No. C2, **1996**, 269.
[33] http://www.xsi.nl, XDAP software, code and licensing, last updated August 2005, last accessed September 2005.
[34] G. E. van Dorssen, D. C. Koningsberger, D. E. Ramaker, *J. Phys. Condens. Matter* **2002**, *14*, 13529.
[35] D. C. Koningsberger, B. L. Mojet, G. E. van Dorssen, D. E. Ramaker, *Top. Catal.* **2000**, *10*, 143.
[36] S. I. Zabinsky, J. J. Rehr, A. Ankudinov, R. C. Albers, M. J. Eller, *Phys. Rev. B* **1995**, *52*, 2995.

  